Journal of Molecular Catalysis A: Chemical 316 (2010) 59–64

Contents lists available at ScienceDirect

Journal of Molecular Catalysis A: Chemical

journal homepage: www.elsevier.com/locate/molcata

Effects of surface area and oxygen vacancies on ceria in CO oxidation: Differences and relationships

Yi Liu, Cun Wen, Yun Guo*, Guanzhong Lu, Yanqin Wang*

Lab for Advanced Materials, Research Institute of Industrial Catalysis, East China University of Science and Technology, Shanghai 200237, PR China

ARTICLE INFO

Article history:
Received 13 August 2009
Received in revised form
30 September 2009
Accepted 30 September 2009
Available online 8 October 2009

Keywords:
CeO_2
Mechanism
Surface area
Oxygen vacancies
Oxygen migration
Rate-determining step
Lattice oxygen extraction

ABSTRACT

Many properties of ceria, such as surface area, defects, and exposed crystal faces, were found to influence the CO oxidation performance of the ceria. Nevertheless, the relations of these properties, which will facilitate the understanding of the catalytic role of ceria in CO oxidation, have not been studied. In this study, the ceria catalysts, HY and CA, were synthesized by hydrothermal method and citric acid sol–gel method, respectively, and the difference in the CO oxidation performance of them was studied using kinetics analysis. Results of temperature-programmed experiments and pulse experiment indicated the lattice oxygen extraction was the rate-determining step (RDS) in the CO oxidation on HY and CA catalysts. The RDS was influenced predominantly by the amount of the active lattice oxygen and the rate of oxygen migration on the catalyst, which were related to the surface area and oxygen vacancies in the catalyst.

1. Introduction

CO is a noxious gas which exists in many industrial procedures. Catalytic oxidation is one of the most effective methods to remove the CO by converting CO to CO_2. Cerium is one of the rare earth elements which show unique catalytic performance because of its 4f electron structure. Ceria has been widely applied as an important co-catalyst in the catalyst for CO oxidation. Many efforts have been paid to understand the catalytic role of the ceria in the CO oxidation [1–5], and the major role of the ceria is attributed to the improved activity and selectivity, and the increased thermal stability.

According to the published literature, many properties of ceria, such as surface area, oxygen vacancy, morphology, and exposed crystal face, are considered as the important factors which influence the catalytic activity of ceria [6–12]. Recently, the investigation of Liu et al. [6] on the ceria nanorods with oxygen vacancy clusters indicated that the larger size oxygen vacancy clusters were responsible for the reducibility and reactivity of the ceria nanorods in CO oxidation. Zhang et al. [9] synthesized $CeO_{2-\delta}$ nanocrystals with controllable sizes and evaluated their catalytic activities for CO oxidation reaction. The improved CO oxidation activity of the $CeO_{2-\delta}$ nanocrystal was attributed to the more oxygen vacancies and larger surface area. Nevertheless, Aneggi et al. [10] investigated the CO oxidation activity of polycrystalline ceria powders and found that pretreating the samples at high temperature enhanced the specific rate of CO oxidation, although the surface area of samples was decreased with the increased temperature. HRTEM analysis revealed that the enhanced activity was attributed to the exposure of the more reactive crystal face (1 0 0) after the pretreatment. Zhou et al. [12] also prepared nano-scaled ceria and found that the polycrystalline assembled ceria nanocrystals (PANs) showed better CO catalytic activity than the nanopolyhedra ceria and the mesoporous ceria. The higher particle dispersity and free of poisonous P impurities on the surface were considered to enhance the CO oxidation activity of PANs.

Nevertheless, these properties, which seem like irrelevant, may correlate with each other in the overall reaction of CO oxidation. For example, the exposed crystal face not only influenced the adsorption properties of ceria [7,13], but also affected the oxygen migration from the subsurface and bulk to the surface [14]. The oxygen vacancies also showed impact on the adsorption for reactants and on the oxygen migration. Thus, both the exposed crystal face and the oxygen vacancies can influence the reaction rate of the adsorption step and the oxygen migration. In this regard, these factors had inner relation because they could influence the specific steps in the CO oxidation together. So, finding the properties which affect the CO oxidation activity of ceria, and finding the relations of

* Corresponding authors. Tel.: +86 21 64253824; fax: +86 21 64253824.
E-mail address: yunguo@ecust.edu.cn (Y. Guo), wangyanqin@ecust.edu.cn (Y. Wang).

1381-1169/$ – see front matter © 2009 Elsevier B.V. All rights reserved.
doi:10.1016/j.molcata.2009.09.022

these properties would enhance the understanding of the catalytic roles of ceria and shed some light on the optimization of the CO oxidation activity of the ceria.

In present work, two ceria catalysts were prepared by the hydrothermal method and citric acid sol–gel method, and the CO oxidation activity of them was investigated. The differences of the CO oxidation activity of these catalysts were studied using the kinetics analysis. The results of temperature-programmed experiment and pulse experiment were used to identify the rate-determining step (RDS) in the CO oxidation reaction on two catalysts. According to the obtained RDS, the relations of the properties of the ceria which predominantly influenced their CO catalytic activities were illustrated.

2. Experimental

2.1. Synthesis

In the hydrothermal method, the raw materials $(NH_4)_2Ce(NO_3)_6$ and urea were dissolved in deionized water. Then, the solution was transferred into a Teflon-lined container, and hydrothermally treated at 130 °C for 4 h with stirring. After cooled down to room temperature, the precipitate was filtered, washed with deionized water and ethanol for several times, and dried at 110 °C. After calcination at 550 °C for 4 h, a pale-yellow powder of CeO_2 was obtained and denoted as HY.

In the citric acid sol–gel method, the raw materials $(NH_4)_2Ce(NO_3)_6$ and citric acid were dissolved in deionized water. Then, the solution was kept at 80 °C with stirring to obtain transparent sol, followed by keeping at 120 °C overnight. After calcination at 550 °C for 4 h, the obtained yellow powder CeO_2 was denoted as CA.

2.2. Characterization

BET specific surface areas (SSAs) of the catalysts were measured by adsorption of N_2 at 77 K using a Quantachrome NOVA 4000e apparatus.

Powder X-ray diffraction (XRD) patterns of catalysts were collected on Rigaku D/max 2550 VB/PC diffractometer using a Cu Kα radiation (λ = 1.54056 Å) in the range $10° \leq 2\theta \leq 80°$. X-ray tube was operated at 40 kV and 100 mA.

Electron paramagnetic resonance (EPR) spectra were recorded with a Bruker EMX-8/2.7 EPR Spectrometer. Equal amounts of the catalysts were placed into the homemade quartz tube with stopcocks. The catalysts were pretreated at 550 °C under He flow for 1 h to remove the impurities, and cooled down to room temperature under the same atmosphere. During experiment, the quartz tube was full of the He atmosphere and sealed. The EPR spectra were recorded at room temperature and calibrated with 2,2-diphenyl-1-picylhydrazyl (g = 2.0036) at the X-band frequency (≈9.7 GHz).

CO-TPD was performed on a quartz tube reactor at atmospheric pressure. Typically 50 mg catalyst was pretreated by He (50 mL/min) at 550 °C for 3 h to remove the impurities. After the system was cooled down to room temperature, the CO flow (30 mL/min) was introduced into the system till the system reached the saturated adsorption. Then the system was purged by the He flow, and the system was heated from room temperature to 550 °C at a heating rate of 10 °C/min. The effluent gas was monitored by an on-line quadrupole mass spectrometer (MS, IPC 400, INFICON Co. Ltd.).

CO_2-TPD was conducted on 50 mg catalyst at atmospheric pressure. The catalyst was pretreated at 550 °C under He flow (50 mL/min) and cooled down to 100 °C to adsorb CO_2. After reached saturated adsorption, the system was purged by the He flow, and the experiment was performed from 100 to 550 °C at a heating rate of 10 °C/min. The effluent gas was monitored by the on-line MS.

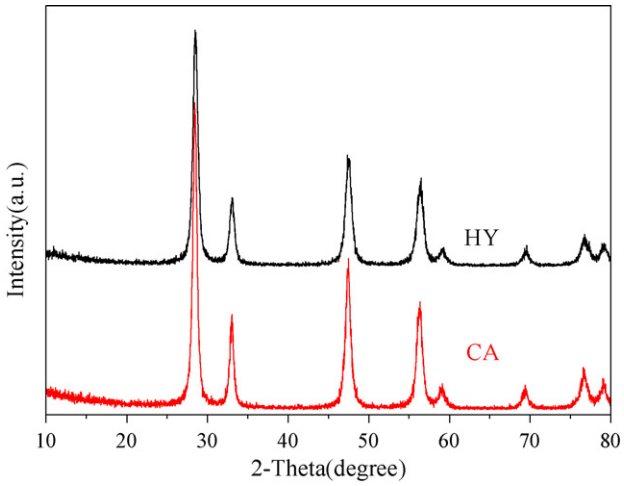

Fig. 1. XRD patterns of CeO_2 samples.

O_2-TPD was conducted on 100 mg catalyst under He flow (50 mL/min). The catalyst was pretreated at 550 °C under He flow followed by treated under O_2 (20 mL/min) at 100 °C. After reached the saturated adsorption, the system was cooled down to room temperature under O_2 flow. Then the system was purged by the He flow, and the O_2-TPD experiment was performed from room temperature to 550 °C at a heating rate of 20 °C/min. The output signal of the effluent gas was monitored by a TCD detector.

CO-TPR was conducted on the quartz tube reactor under 10% CO/He flow (50 mL/min). Before experiment, the catalyst was pretreated at 550 °C for 3 h under He flow, and cooled down to room temperature. Then, the TPR experiment was performed under the 10% CO/He flow at a heating rate of 10 °C/min from room temperature to 550 °C. The effluent gas was monitored by the on-line MS.

The CO pulse experiments were conducted on the quartz tube reactor and the effluent gas was monitored by the on-line MS. Catalyst (50 mg) was pretreated at 550 °C for 3 h under a flow of He (30 mL/min), followed by cooling down to 400 °C at the same atmosphere. After the system reached the equilibrium, 35.62% CO/Ar was pulsed into the system at an interval of 30 s with a loop volume of 73.7 μL. Argon was used as the calibration diluents.

CO oxidation reaction was conducted at atmospheric pressure with a heating rate of 5 °C/min. The typical feed conditions were 2% CO, 20% O_2, and Ar as diluents, with a total flow rate of 100 mL/min. Catalyst (100 mg, 40–60 mesh) was put into the quartz tube reactor, and a thermocouple was used to monitor the catalyst bed temperature. The CO conversion was analyzed by a gas chromatography equipped with a TCD detector.

3. Results

3.1. Surface area and structure

The BET surface areas of HY and CA catalysts are 63.2 and 26.3 m^2/g, respectively. The structure of the catalyst was characterized by XRD and shown in Fig. 1. The diffraction patterns indicate that both catalysts are the cubic fluorite type CeO_2 crystals with the space group $Fm3m$ (JCPDS 65-2975). The refinement of the XRD patterns in Fig. 1 shows that the lattice parameters of HY and CA are identical. On the other hand, the full widths at half-maximum

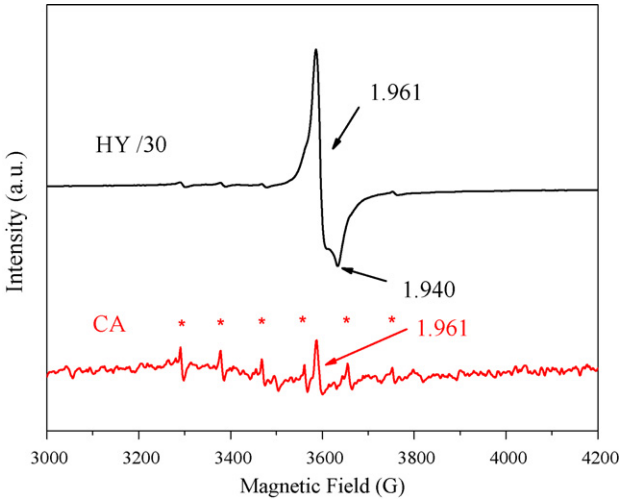

Fig. 2. EPR spectra of CeO_2 samples collected at room temperature.

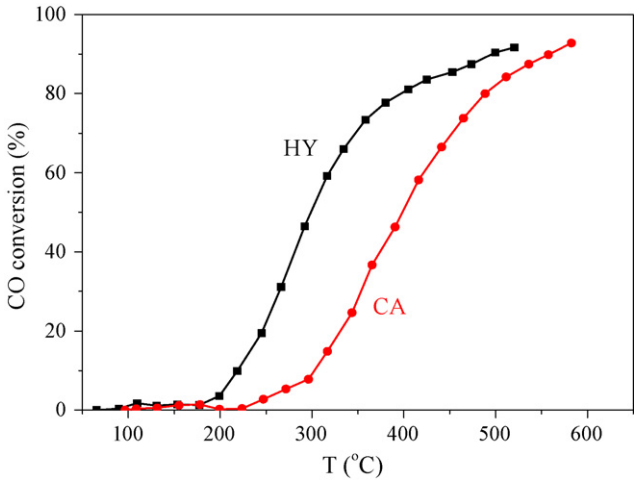

Fig. 3. CO conversions as a function of temperature on HY (square) and on CA (circle).

of the diffraction peaks on CA catalyst are narrower than that on HY catalyst, which shows the crystallization degree of CA catalyst is better than that of HY catalyst. Calculated by adopting Scherrer equation, the grain sizes of (1 1 1) plane of HY and CA are 12.1 and 13.6 nm, respectively. The smaller grain size of HY may be related to the higher BET surface area.

3.2. EPR

EPR experiment was conducted to investigate the fine structure of the ceria catalysts. The EPR spectra of the HY and CA catalysts are shown in Fig. 2. On both catalysts, a six-line hyperfine structure marked with asterisk is the paramagnetic signal of Mn^{2+} impurity [15]. The inductively coupled plasma atomic emission spectrometer (ICP-AES) analysis shows that the Mn^{n+} concentrations in HY and CA are 3.0 and 50.0 ppm, respectively. The spectrum of HY catalyst shows a strong paramagnetic signal at $g \sim 1.961$ and $g \sim 1.940$, but the signal intensity at the same location is very weak on CA catalyst. This signal is usually attributed to the Ce^{3+} species in ceria which should be detected by EPR at very low temperature (no higher than 77 K) because the higher temperature would broaden the EPR lines to beyond detection limits [16]. But, some researchers reported that the asymmetrical lattice environment of Ce^{3+} species would make the EPR signal measurable [5,17–19]. Therefore, the detected paramagnetic signals at $g \sim 1.961$ and $g \sim 1.940$ are attributed to the Ce^{3+} species with a distorted symmetry on the surface [20]. Because the Ce^{3+} signal is intrinsic to the corresponding oxygen vacancies in ceria, thus the stronger intensity of this signal on HY demonstrates that the HY catalyst has more oxygen vacancies on the surface than the CA catalyst.

3.3. CO oxidation

The CO catalytic activities of the two catalysts are exhibited in Fig. 3. HY catalyst can convert more CO than CA catalyst at the same temperature. The T_{50} (the temperature when CO conversion reached 50%) on HY catalyst is lower than that on CA catalyst for 99 °C, and the T_{90} (temperature at which the CO conversion reached 90%) on the former is lower than that on the latter for 62 °C. These differences indicate that HY catalyst has better CO catalytic activity than CA catalyst. In order to study the effect of the specific factors of ceria in the individual steps contained in overall reaction, following experiments were conducted because many factors can influence the CO catalytic activity of ceria. First of all, the adsorption properties of the catalysts toward reactive molecules were investigated.

3.4. CO-TPD

CO-TPD experiment was conducted to investigate the properties of CO adsorption on the HY and CA catalysts. The CO_2 evolution curves during CO-TPD are shown in Fig. 4. On HY, there is a strong band located at 126 °C, and a broad band appears at about 370 °C. Similarly, two bands of CO_2 desorption are observed on CA at 126 °C and at about 370 °C. Additionally, two shoulder peaks are observed on CA at both sides of the band which is centered at 126 °C. The appearance of CO_2 signal on two catalysts means that both HY and CA can adsorb CO at room temperature. The extra CO_2 desorption bands on CA indicate that CA has more kinds of CO adsorption sites than HY.

3.5. CO_2-TPD

The properties of CO_2 desorption on HY and CA catalysts were studied by the CO_2-TPD. The MS signals of the CO_2 desorption are exhibited in Fig. 5. The desorption curves show that there are two strong desorption peaks below 200 °C on both catalysts, centered at 147 and 178 °C. But the intensity of the CO_2 desorption signal on HY

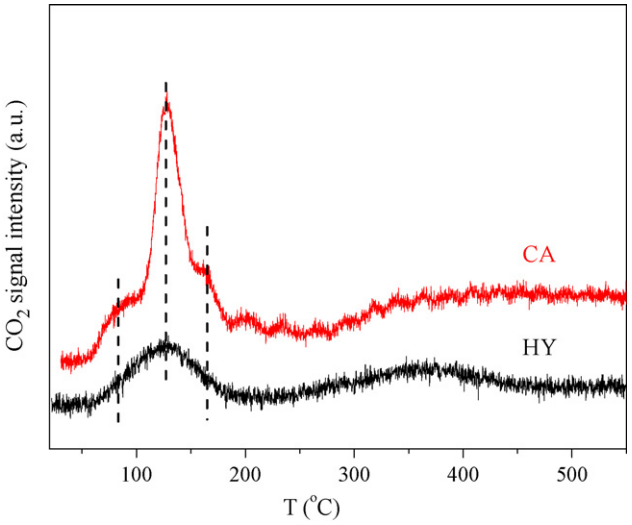

Fig. 4. CO_2 evolution curves (MS) on HY and CA during CO-TPD.

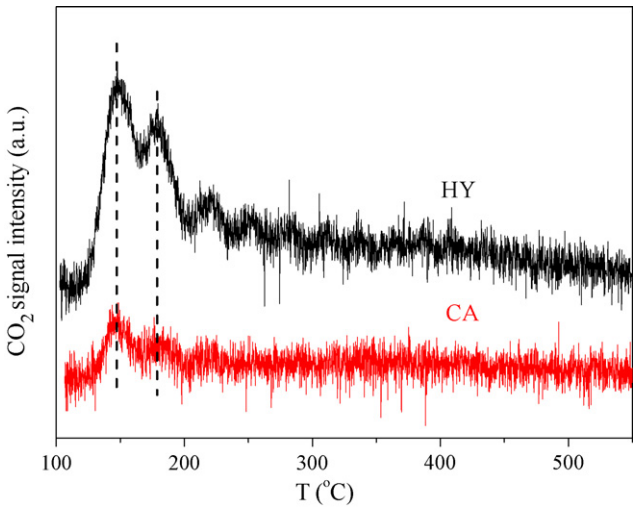

Fig. 5. CO_2 desorption signals (MS) on HY and CA during CO_2-TPD.

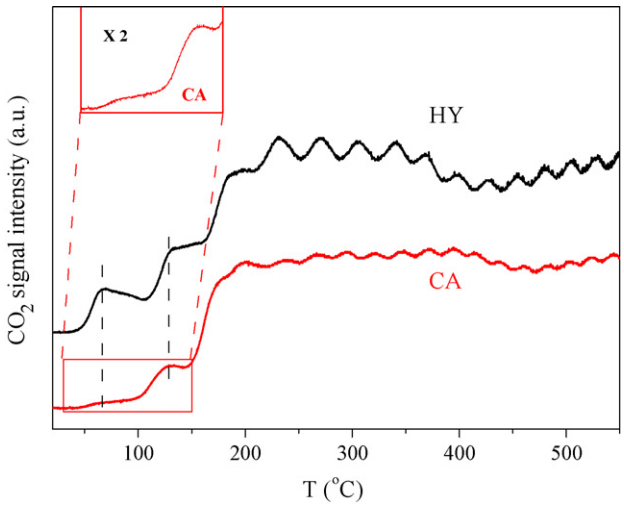

Fig. 7. CO_2 evolution curves (MS) on HY and CA during CO-TPR.

is much stronger than that on CA. These phenomena demonstrate that the adsorption strength of CO_2 on HY is similar to that on CA, but HY has more CO_2 adsorption sites than CA.

3.6. O_2-TPD

In order to investigate the properties of gas phase oxygen adsorption on HY and CA, O_2-TPD experiment was performed. The desorption curve (shown in Fig. 6) on HY shows that there are two weak desorption peaks centered at 260 and 355 °C, besides the strong desorption peak at 149 °C. The desorption curve on CA also has three desorption peaks, located at 147, 260, and 367 °C. These phenomena demonstrate that the O_2 adsorption properties of the two catalysts are different at the temperature range higher than 300 °C. The higher desorption temperature for O_2 on CA (above 300 °C) means that the interaction between CA and the gas phase oxygen is stronger than that between HY and the gas phase oxygen. That is to say, CA exhibits stronger adsorption properties for gas phase oxygen than HY.

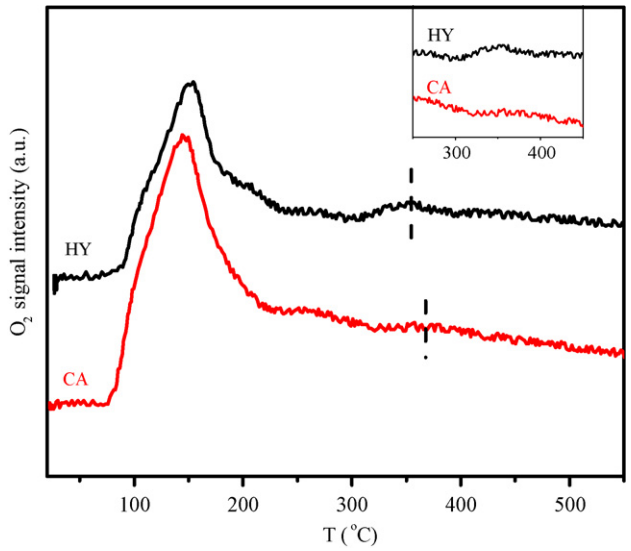

Fig. 6. O_2 desorption curves on HY and CA during O_2-TPD. (Insert figure was the O_2 desorption curves in the range of 250–450 °C.)

3.7. CO-TPR

Catalyst properties not only influence the adsorption properties for reactants and the desorption properties for products, but also have impacts on the rate of the reaction between reactants and catalysts. Following CO-TPR experiment was conducted to study the reactivity of the catalysts toward CO. The evolved CO_2 curves during CO-TPR are shown in Fig. 7. On both catalysts, CO_2 can be produced at very low temperature (below 40 °C). These phenomena indicate that HY and CA have good reducibility. And the similar CO_2 evolution curves on two catalysts illustrate that the reducibility of them is very similar. Additionally, the slightly stronger intensity of the CO_2 signal on HY means that HY has more amount of active lattice oxygen than CA.

3.8. CO pulse

Besides the reducibility and the lattice oxygen amount of ceria, oxygen migration rate is also an important property of ceria for the reaction between the catalysts and CO. The oxygen migration in HY and CA was investigated by the CO pulse experiment. The signals of 28 (m/z) represent CO, and are shown in Fig. 8. The intensity of the signal 28 at the first pulse on HY is lower than that on CA, which

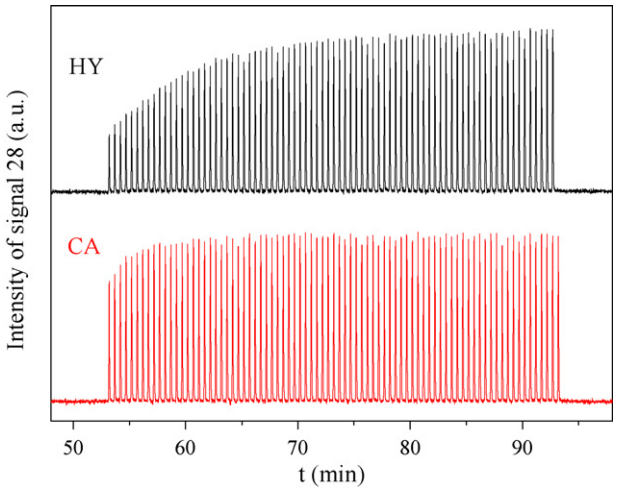

Fig. 8. Signal 28 during CO pulse experiment at 400 °C on HY and CA, which was monitored by on-line MS at reactor outlet.

indicates that more CO was converted by HY. This result further verifies the results in CO-TPR that HY has more amount of the active lattice oxygen per gram than CA. After the first pulse, the pulsed CO is mainly converted by the lattice oxygen which migrates from the subsurface and/or the bulk of ceria. The slope of the CO signal change is slightly mild on HY than on CA. This different slope may be induced by the different amount of the active lattice oxygen and/or the rate of oxygen migration. As mentioned in the CO-TPR section, HY has more amount of the active lattice oxygen than CA. If the CO conversion during the CO pulse experiment is predominantly influenced by the amount of the active lattice oxygen (that is to say, two catalysts have a similar oxygen migration rate), the ratio of the migrated lattice oxygen amount on HY to that on CA should keep constant at each pulse, and the trends of the CO consumption on both catalysts should show similar slopes. Nevertheless, neither the ratio nor the slopes of the CO consumption on HY and on CA keep constant, which demonstrates that the oxygen migration rate also influences the results of the CO pulse experiment in addition to the amount of the active lattice oxygen. The results in Fig. 8 elucidate that at each pulse interval, more oxygen can migrate from the inner part of HY than that of CA, which indicates that the rate of the oxygen migration in HY is faster than that in CA.

4. Discussion

CO oxidation test (Fig. 3) shows that HY has better CO oxidation activity. The difference in the CO oxidation activities of HY and CA cannot be attributed to the existence of the Mn^{2+} impurity, because the Mn^{n+} concentrations in the catalysts are very low. At the same time, the Mn^{n+} concentrations which are determined by ICP-AES cannot be related to the CO oxidation activities of the catalysts. Furthermore, the Mn^{n+} impurity is not doped into the ceria lattice, because the lattice parameters of HY and CA are identical. These results indicate that the Mn^{n+} impurities are not in the catalyst lattice and these impurities do not primarily influence the CO oxidation activity of the catalysts. On the other hand, the Mn^{n+} concentrations determined by the ICP-AES are not consistent with the signals of Mn^{2+} shown in the EPR spectra. This inconsistent phenomenon indicates that the Mn impurities may exist as some other forms beside Mn^{2+}, which do not have paramagnetic signal in the EPR spectra.

In order to identify the factors which influence the CO oxidation activity, the reaction mechanism of CO oxidation should be understood. It has been reported that the CO oxidation on ceria follows Mars-van Krevelen mechanism [7,21]. In this mechanism, the ceria experiences a redox cycle, which means the ceria is reduced by CO at first, and immediately oxidized by gas phase oxygen in feed gases. The main steps in the CO oxidation are expressed as follows [22]:

$$CO + * \rightarrow CO* \quad (1)$$

$$CO* + O_L \rightarrow COO_L* \quad (2)$$

$$COO_L* \rightarrow CO_2 + V_L + * \quad (3)$$

$$O_2 + V_L \rightarrow 2O_L \quad (4)$$

Here, "*" represents adsorption sites on the surface, and the species with this suffix means the corresponding adsorption species. "O_L" and "V_L" are denoted as the lattice oxygen and the oxygen vacancies in ceria, respectively. Eq. (1) describes the process of CO adsorption on the ceria surface. These adsorbed CO reacts with the lattice oxygen to form reaction intermediates (Eq. (2)). With the desorption of the reaction intermediates, CO_2 and the oxygen vacancies are produced and the adsorption sites are refreshed (Eq. (3)). Simultaneously, the gas phase oxygen is activated on the catalyst to replenish the oxygen vacancies (Eq. (4)). Thus, the catalyst is refreshed by this redox cycle. Results in Fig. 3 indicate that HY has better CO catalytic oxidation performance than CA. Following experiments were conducted to investigate the different performance of the catalysts in related steps.

In CO-TPD experiment (Fig. 4), the produced CO_2 signals indicate that both catalysts can adsorb CO at room temperature. On the other hand, the extra shoulder peaks on CA indicate that more kinds of the CO adsorption sites exist on CA than that on HY. The differences in the CO adsorption properties can be attributed to the different surface properties of the catalysts. HY has more oxygen vacancies on the surface, revealed by the analyses of XRD and EPR, which indicates that the ratio of the Ce^{3+}/Ce^{4+} ions on HY is higher than that on CA. The unpaired electrons on the Ce^{3+} ions would make HY surface shows slightly electron-rich state than CA, and this electron-rich surface would produce electrostatic repulsion for the CO adsorption, because there is a lone pair of electrons on the carbon orbital of the CO molecules [23,24]. Nevertheless, the more kinds of the CO adsorption sites on CA does not make CA shows the better CO oxidation activity than HY. This result indicates that the properties of the CO adsorption do not predominantly influence the CO oxidation performance.

Besides the CO adsorption properties, the differences in the CO_2 desorption properties between HY and CA are shown in Fig. 5. The similar curves of the CO_2 desorption on HY and CA catalysts indicate that two catalysts have the similar CO_2 adsorption strength. On the other hand, the intensity of the CO_2 desorption signal on HY is higher than that on CA, which shows that HY can adsorb more CO_2. This phenomenon indicates that more oxygen vacancies exist on the HY surface, because the surface defect sites of the metal oxides facilitate the CO_2 adsorption [25,26]. At the same time, the more amount of CO_2 adsorption on HY does not make HY show worse catalytic performance than CA, which indicates that the properties of the CO_2 desorption in Eq. (3) do not primarily influence the CO oxidation activity.

Besides the properties of the CO adsorption and the CO_2 desorption, the oxygen adsorption properties were also investigated. In Mars-van Krevelen mechanism, the oxygen vacancies which are created by the reaction between the adsorbed CO and the lattice oxygen can be replenished by the gas phase oxygen. The desorption curves during O_2-TPD (Fig. 6) indicate that the interaction between the catalysts and the gas phase oxygen is different on two catalysts. The desorption peak at high temperature range (above 300 °C) on HY appears at relatively lower temperature than that on CA, which demonstrates that the O_2 adsorption on HY is weaker than that on CA. According to the reported results [7], the defects on ceria surface should favor the adsorption of O_2 molecules. But in this work, more oxygen vacancies on HY surface do not enhance the O_2 adsorption ability of HY. This phenomenon may be attributed to the electrostatic repulsive effect between the slightly electron-rich HY surface and the lone pair electrons on the O_2 molecules, which influence the O_2 adsorption. Although the different desorption peak on the catalysts indicates that CA has better ability to adsorb gas phase oxygen, the CO oxidation activity of CA is lower than that of HY. Thus, the properties of the O_2 adsorption do not primarily control the catalytic performance of the HY and CA catalysts.

According to the Mars-van Krevelen mechanism, the lattice oxygen takes part in the CO oxidation. The reaction between the lattice oxygen and the CO was studied by the CO-TPR and the CO pulse experiment. In Fig. 7, CO_2 can be formed at similar temperature on HY and CA. Above discussions in the CO-TPD and the CO_2-TPD have indicated that both catalysts can adsorb CO readily and the CO_2 desorption property of them is also similar. Therefore, the properties of CO adsorption and CO_2 desorption do not influence the CO_2 evolution curves in the CO-TPR, and the reducibility would affect the CO_2 evolution curves. The similar CO_2 evolution curves during the CO-TPR illustrate that both catalysts have the similar reducibil-

ity, and HY has more amount of the active lattice oxygen than CA. The results in CO pulse also verify that HY has more amount of the active lattice oxygen.

Furthermore, the results of the CO pulse experiment (Fig. 8) show the difference in oxygen migration properties of two catalysts. This oxygen migration property is also considered to be responsible for the catalytic performance of the CO oxidation on HY and CA. This is because in the overall reaction, the oxygen vacancies, which are produced after lattice oxygen extraction, should be replenished based on the Mars-van Krevelen mechanism. The oxygen vacancies can be replenished by gas phase oxygen and/or inner lattice oxygen. Results of the O_2-TPD have indicated that the interaction between the catalyst and the O_2 molecules do not predominantly influence the CO oxidation activity. Thus the faster oxygen migration enhances the CO oxidation performance of HY. One may argue that although different oxygen migration rates are observed in CO pulse, it seems like the CO_2 evolution curves in CO-TPR are not influenced by the oxygen migration properties. Giordano et al. [27] used a cell model to study the effects of oxygen migration in the TPR results of the ceria, and indicated that the contribution of the oxygen migration to the shape of the TPR curves is negligible. So, in this study, the difference in the oxygen migration properties is just be observed in the CO pulse experiment.

Above results indicate that the different properties of the catalysts in the corresponding steps expressed in Eqs. (1), (3) and (4) do not show dominant impacts on the CO oxidation activity of HY and CA. But the results in the CO-TPR and the CO pulse experiment show that there is a positive relation between the active lattice oxygen amount or the oxygen migration rate and the CO oxidation activity of HY and CA. The results further elucidate that both the amount of the active lattice oxygen and the oxygen migration rate influence the rate of lattice oxygen extraction in CO oxidation. Therefore, the lattice oxygen extraction (expressed in Eq. (2)) is the RDS in the CO oxidation on HY and CA catalysts. More amount of the active lattice oxygen and faster oxygen migration enhance the CO catalytic activity of HY by accelerating the RDS. For HY and CA, the more amount of active lattice oxygen is related to the larger surface area, and the oxygen migration rate is improved by more oxygen vacancies on HY surface.

In order to further verify this result, the commercial ceria (CC), purchased from Sinopharm Chemical Reagent Co. Ltd. (Shanghai, PR China) was used as a reference catalyst. The BET surface area of the CC catalyst is very small (1.4 m^2/g) and the EPR spectra in Fig. A1 shows that the intensity of the Ce^{3+} signal on the CC catalyst is much weaker than those on HY and CA catalysts. The CO oxidation test shows that the T_{50} and T_{90} of the CC catalyst are 547.7 and 673.8 °C, respectively, much higher than those of HY and CA, indicating that CC is the worst catalysts for CO oxidation. This result further comfirms that the activity of ceria on CO oxidation is determined by surface area and oxygen vacancies.

5. Conclusion

In this study, the detailed mechanism of the CO oxidation on HY and CA was investigated. The analyses elucidate that the lattice oxygen extraction is the RDS in the CO oxidation. The amount of the active lattice oxygen and the oxygen migration rate influence the reaction rate of the lattice oxygen extraction and further affect the CO oxidation activity of HY and CA. Meanwhile, in the tested catalysts, the amount of the active lattice oxygen and the oxygen migration rate are related to the surface area and the surface oxygen vacancies, respectively.

The results reported here indicate that the surface area and the surface oxygen vacancies in the ceria can influence the CO oxidation performance together, because both factors play dominant role in the RDS. According to these results, various factors, which have been reported to be responsible for the CO catalytic performance of ceria, may reach a consensus because they may have inner relations in specific steps in the CO oxidation.

Acknowledgments

This project was supported financially by the National Basic Research Program of China (No. 2004CB719500), the National Natural Science Foundation of China (Nos. 20601008 and 20673037), the New Century Excellent Talents in University (NCET-05-415), and Commission of Science and Technology of Shanghai Municipality (08JC1407900), China.

Appendix A. Supplementary data

Supplementary data associated with this article can be found, in the online version, at doi:10.1016/j.molcata.2009.09.022.

References

[1] J.R. González-Velasco, M.A. Gutiérrez-Ortiz, J.L. Marc, J.A. Botas, M.P. González-Marcos, G. Blanchard, Top. Catal. 16/17 (2001) 101–106.
[2] J. Kašpar, P. Fornasiero, N. Hickey, Catal. Today 77 (2003) 419–449.
[3] R. Rajasree, J.H.B.J. Hoebink, J.C. Schouten, J. Catal. 223 (2004) 36–43.
[4] R.H. Nibbelke, M.A.J. Campman, J.H.B.J. Hoebink, G.B. Marin, J. Catal. 171 (1997) 358–373.
[5] P. Ratnasamy, D. Srinivas, C.V.V. Satyanarayana, P. Manikandan, R.S. Senthil Kumaran, M. Sachin, V.N. Shetti, J. Catal. 221 (2004) 455–465.
[6] X.W. Liu, K.B. Zhou, L. Wang, B.Y. Wang, Y.D. Li, J. Am. Chem. Soc. 131 (2009) 3140–3141.
[7] C.T. Campbell, C.H.F. Peden, Science 309 (2005) 713–714.
[8] C.J. Zhang, A. Michaelides, D.A. King, S.J. Jenkins, Phys. Rev. B 79 (2009) 075433.
[9] Y.-W. Zhang, R. Si, C.-S. Liao, C.-H. Yan, C.-X. Xiao, Y. Kou, J. Phys. Chem. B 107 (2003) 10159–10167.
[10] E. Aneggi, J. Llorca, M. Boaro, A. Trovarelli, J. Catal. 234 (2005) 88–95.
[11] K.B. Zhou, X. Wang, X.M. Sun, Q. Peng, Y.D. Li, J. Catal. 229 (2005) 206–212.
[12] H.-P. Zhou, Y.-W. Zhang, R. Si, L.-S. Zhang, W.-G. Song, C.-H. Yan, J. Phys. Chem. C 112 (2008) 20366–20374.
[13] B. Herschend, M. Baudin, K. Hermansson, Chem. Phys. 328 (2006) 345–353.
[14] H. Cordatos, T. Bunluesin, J. Stubenrauch, J.M. Vohs, R.J. Gorte, J. Phys. Chem. 100 (1996) 785–789.
[15] A. Martínez-Arias, M. Fernández-Garcia, L.N. Salamanca, R.X. Valenzuela, J.C. Conesa, J. Soria, J. Phys. Chem. B 104 (2000) 4038–4046.
[16] A. Trovarelli (Ed.), Catalytic Science Series: Catalysis by Ceria and Related Materials, Imperial College Press, London, 2002, pp. 169–171.
[17] C. Oliva, G. Termignone, F.P. Vatti, L. Forni, A.V. Vishniakov, J. Mater. Sci. 31 (1996) 6333–6338.
[18] N. Sergent, J.F. Lamonier, A. Aboukaïs, Chem. Mater. 12 (2000) 3830–3835.
[19] P.G. Harrison, I.K. Ball, W. Azelee, W. Daniell, D. Goldfarb, Chem. Mater. 12 (2000) 3715–3725.
[20] E. Abi-aad, R. Bechara, J. Grimblot, A. Aboukaïs, Chem. Mater. 5 (1993) 793–797.
[21] M. Huang, S. Fabris, J. Phys. Chem. C 112 (2008) 8643–8648.
[22] M.W. Zhao, M.Q. Shen, J. Wang, J. Catal. 248 (2007) 258–267.
[23] G. Blyholder, J. Phys. Chem. 68 (1964) 2772–2778.
[24] Z.X. Yang, T.K. Woo, K. Hermansson, Chem. Phys. Lett. 396 (2004) 384–392.
[25] Z.X. Song, W. Liu, H. Nishiguchi, Catal. Commun. 8 (2007) 725–730.
[26] H. Tsuji, A. Okamura-Yoshida, T. Shishido, H. Hattori, Langmuir 19 (2003) 8793–8800.
[27] F. Giordano, A. Trovarelli, C. de Leitenburg, G. Dolcetti, M. Giona, Ind. Eng. Chem. Res. 40 (2001) 4828–4835.